

Quantum cluster kink and ring frustration

Zhen-Yu Zheng, Han-Chuan Kou, and Peng Li

*College of Physics, Sichuan University, 610064, Chengdu, People's Republic of China
and Key Laboratory of High Energy Density Physics and Technology of Ministry of Education,
Sichuan University, 610064, Chengdu, People's Republic of China*

(Dated: March 31, 2025)

In this paper, we work on the pure and mixed cluster models with periodic boundary condition. The first purpose is to establish the concept of quantum cluster kink. Simple pictures are easily constructed in the pure cluster model. We clarify that there are two types of cluster kinks since there are two types of ground states depending on the cluster length, of which the first type exhibits symmetry breaking order and the second one exhibits string order. Based on the pictures, cluster kink number and its density are defined, which are very useful in describing the quantum phase transitions in the mixed cluster model. Cluster kinks deriving from different sources can coexist, compete with each other, and lead to quantum phase transitions. The second purpose is to elucidate that the effect of ring frustration can be realized in the cluster model with symmetry breaking order. Because the geometrical ring frustration results in a huge ground-state degeneracy in the pure cluster model and induces a special extended-kink phase with gapless excitations in the mixed cluster model. And, although the ring frustration does not change the phase transition point, it brings a nonlocal scaling factor to the correlation function and double the number of lowest eigenvalues in the entanglement spectrum for the extended-kink phases.

I. INTRODUCTION

Kinks (or domain walls) play important roles in the field of condensed-matter physics [1, 2]. The simplest kink is the one in a classical Ising chain which is a consequence of thermal fluctuations. But the scenario can be generalized to quantum spin chains, which is taken as a consequence of quantum fluctuations. Moreover, quantum phase transition can be induced when the kinks become more and more pervasive in the ground state. The quantum critical point can be reflected by the dynamics of kinks through Kibble-Zurek mechanism [3–8]. Various types of kinks can be introduced according to the underlying models for practical problems ranging from magnetism [9] to other research fields [10].

Recently, a family of cluster models have attracted lots of attention on the topics of symmetry protected topology and topological quantum computation [11–26]. In this work, we demonstrate that a general concept of quantum cluster kink can be established for these models. Basing on this concept, useful quantities, kink number and its density, can be defined and worked out to describe quantum phase transitions. More important, it turns out that there are two types of cluster kinks, of which one can provide the playground for exploring the effect of ring frustration [27–33].

The paper is organized as follows. In Sec. II, we establish the concept and picture of quantum cluster kink in an exact manner basing on the pure cluster Hamiltonian. Two types of kinks are introduced. The useful quantities, cluster kink number and its density, are defined. And the condition for realizing ring frustration is elucidated. In Sec. III, we work on a mixed cluster model, which can possess a peculiar gapless extended-kink phase as an effect of ring frustration. The phase diagrams containing extended-kink phases are plotted. The density of kink

number is shown to be a useful quantity for reflecting the competing orders in the ground states. Its second derivative exhibits a divergent peak at the critical point, whose scaling behavior has an interesting relation with the one of the second derivative of the ground-state energy density. The influences of ring frustration in the correlation function and entanglement spectrum are exemplified. At last, in Sec. IV, we give brief summary and some discussions.

II. PURE CLUSTER MODEL

In this section, we focus on the pure xzx - m -cluster Hamiltonian with PBC ($N \gg m$),

$$H_m^{xzx} = J \sum_{j=1}^N \sigma_j^x \tau_{m,j}^z \sigma_{j+m}^x. \quad (1)$$

where $\tau_{m,j}^z = \sigma_{j+1}^z \cdots \sigma_{j+m-1}^z$, the integer m denotes the length of cluster interaction in each term. This Hamiltonian can be called ferro-cluster (FC) for $J < 0$ and antiferro-cluster (AFC) for $J > 0$ respectively.

It is noteworthy, in the classical Ising case ($m = 1$), the system returns to the familiar form, $H_1^{xzx} \equiv H^{\text{Ising}} = J \sum_{j=1}^N \sigma_j^x \sigma_{j+1}^x$, which exhibits ferromagnetic (FM) order for $J < 0$ and antiferromagnetic (AFM) order for $J > 0$ correspondingly. Both orders break the \mathbb{Z}_2 symmetry of the Ising Hamiltonian.

For cases with $m > 1$, the Hamiltonians are of quantum nature. It has been disclosed that the oddity of m can influence the physical properties of the system [26]. We shall disclose the condition for realizing the effect of ring frustration by establishing the concept of quantum cluster kink.

A. Quaternary Jordan-Wigner mapping

The Hamiltonian in Eq. (1) with general m can be easily handled by Jordan-Wigner transformation,

$$c_j^\dagger = \frac{1}{2}(\sigma_j^x + i\sigma_j^y) \prod_{l=1}^{j-1} (-\sigma_l^z). \quad (2)$$

But please notice the faithful *quaternary Jordan-Wigner mapping* (QJWM) should be applied due to the presence of PBC. The complete mapping involves four Hamiltonians and can be pictorially expressed as [30].

$$H_m^c = \begin{array}{c} \boxed{H_m^{xxx}} \\ \swarrow \quad \searrow \\ \boxed{P_z^- H_m^c} \quad \boxed{P_z^+ \tilde{H}_m^c} \\ + \quad + \\ P_z^+ H_m^c \quad P_z^- \tilde{H}_m^c = \tilde{H}_m^c. \\ \searrow \quad \swarrow \\ \tilde{H}_m^{xxx} \end{array} \quad (3)$$

This mapping tells us the solution of H_m^{xxx} can be decomposed into two fermion parity channels as,

$$H_m^{xxx} = P_z^- H_m^c + P_z^+ \tilde{H}_m^c, \quad (4)$$

where the fermion Hamiltonian with PBC ($c_{j+N} = c_j$) reads

$$H_m^c = (-1)^m J \sum_{j=1}^N (c_j - c_j^\dagger)(c_{j+m} + c_{j+m}^\dagger), \quad (5)$$

while \tilde{H}_m^c is a concomitant one with anti-PBC ($c_{j+N} = -c_j$). The parity projectors read

$$P_z^\pm = \frac{1}{2}(1 \pm \mathcal{P}_z), \quad (6)$$

with

$$\mathcal{P}_z = \exp(i\pi M_z), \quad (7)$$

$$M_z = \sum_{j=1}^N \frac{1 + \sigma_j^z}{2} = \sum_{j=1}^N c_j^\dagger c_j. \quad (8)$$

It is noteworthy that the redundant degrees of freedom of H_m^c and \tilde{H}_m^c constitute the ones of \tilde{H}_m^{xxx} as $\tilde{H}_m^{xxx} = P_z^+ H_m^c + P_z^- \tilde{H}_m^c$, which is also a pure xxx -cluster Hamiltonian but with anti-PBC.

B. Picture of cluster kinks: symmetry breaking order and string order

For general m , we can introduce a set of stabilizers for the ground state(s),

$$S_j = \begin{cases} \sigma_j^x \tau_{m,j}^z \sigma_{j+m}^x & (J < 0, \text{ FC case}), \\ -\sigma_j^x \tau_{m,j}^z \sigma_{j+m}^x & (J > 0, \text{ AFC case}). \end{cases} \quad (9)$$

where the dependence of S_j on m is omitted for abbreviation. Usually, the ground state $|E_0\rangle$ is ordered and can be labelled by a set of uniform values $+1$,

$$S_j |E_0\rangle = + |E_0\rangle \quad \forall j. \quad (10)$$

However, in the excited states, some values of stabilizers deviate from $+1$ to -1 . When this occurs, we say *cluster kinks* are created.

There is a distinct difference between the two cases, odd and even m [15, 26]. For $m \in \text{odd}$, the doubly degenerate ground states exhibit \mathbb{Z}_2 symmetry breaking order, just like the classical Ising case ($m = 1$). While for $m \in \text{even}$, the unique ground state exhibits a string order without symmetry breaking.

Here, we draw the same conclusion naturally basing on the string of stabilizers ($r > m$),

$$\mathbb{S}_{j,r} = S_j S_{j+1} \cdots S_{j+r-m}. \quad (11)$$

The pictures for two types of cluster kinks can be established subsequently. And we shall demonstrate that both types of cluster kinks can be faithfully labelled by the values of stabilizers.

1. Type I cluster kink

For $m \in \text{odd}$, one can find that the string of stabilizers breaks into two disjoint local parts,

$$\mathbb{S}_{j,r} = [-\text{sgn}(J)]^r \mathcal{O}_j^{xy} \mathcal{O}_{j+r-m+1}^{xy}, \quad (12)$$

where each part is a combined spin operator,

$$\mathcal{O}_j^{xy} = \sigma_j^x \sigma_{j+1}^y \cdots \sigma_{j+m-1}^x. \quad (13)$$

We also omit the dependence of $\mathbb{S}_{j,r}$ and \mathcal{O}_j^{xy} on m for abbreviation. Basing on the fact that the operator \mathcal{O}_j^{xy} takes two possible eigenvalues, ± 1 , we define a correlation function for the ground state,

$$C^I(r) = [-\text{sgn}(J)]^r \langle \mathbb{S}_{j,r} \rangle = \langle \mathcal{O}_j^{xy} \mathcal{O}_{j+r-m+1}^{xy} \rangle, \quad (14)$$

and the order parameter

$$\langle \mathcal{O}_j^{xy} \rangle = \sqrt{|C^I(r)|}, \quad (15)$$

to capture the \mathbb{Z}_2 symmetry breaking from the point of view of spin operators [34]. Because we have $\langle \mathbb{S}_{j,r} \rangle = +1$ for the ordered ground states of the pure cluster Hamiltonian in Eq. (1), we get a simple result, $C^I(r) = [-\text{sgn}(J)]^r$. In the Ising case, the definition of correlation function returns to the familiar form,

$$C^I(r) = \langle \sigma_j^x \sigma_{j+r}^x \rangle, \quad (16)$$

and the order parameter is usually marked by $\langle \sigma_j^x \rangle$.

Basing on the local order parameter, we can construct the picture for the cluster kink in the cases with $m \in$

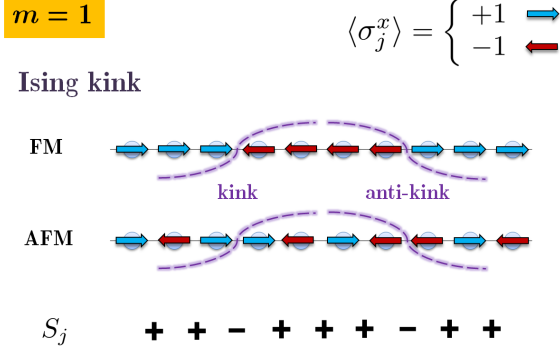


FIG. 1. Ising kink. The picture basing on stabilizers S_j is consistent with the one basing on the local order parameter $\langle \sigma_j^x \rangle$.

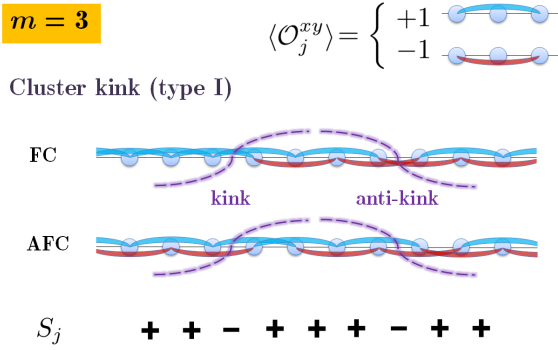


FIG. 2. Type I cluster kink. Similar to the Ising case, the picture basing on stabilizers is consistent with the one basing on local order parameter $\langle \mathcal{O}_j^{xy} \rangle$.

odd. As the simplest example, let us see the picture of Ising kink as shown in Fig. 1. We see that the picture basing on the stabilizers is consistent with the usual picture basing on order parameters. The picture for $m = 3$ is illustrated in Fig. 2, which is a direct generalization of the Ising case in Fig. 1. There are kink and anti-kink pairs in type I cluster kink.

2. Type II cluster kink

For $m \in \text{even}$, the string can not be taken apart. For example, for $m = 2$, we get

$$\mathbb{S}_{j,r} = [\text{sgn}(J)]^{r-3} \sigma_j^x \sigma_{j+1}^y (\sigma_{j+2}^z \cdots \sigma_{j+r-2}^z) \sigma_{j+r-1}^y \sigma_{j+r}^x. \quad (17)$$

This means that one can not find a local order parameter from the point of view of spin operators and has to introduce a nonlocal string order that is represented by the whole string correlation function,

$$C^{\text{II}}(r) = [\text{sgn}(J)]^{r-1} \langle \mathbb{S}_{j,r} \rangle, \quad (18)$$

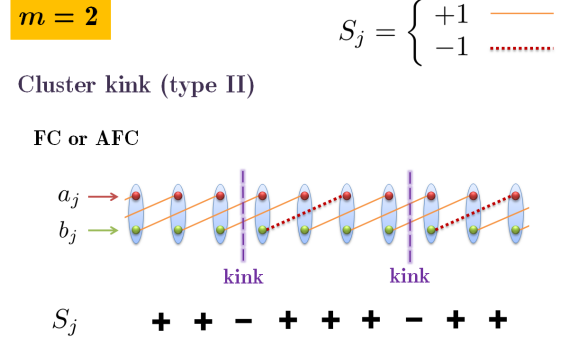


FIG. 3. Type II cluster kink. The picture basing on stabilizers is consistent with the one basing on Majorana fermions. The relation between stabilizers and Majorana fermions can be found in Eq. (19).

which gives almost the same definition in previous studies [15, 22]. Because we have $\langle \mathbb{S}_{j,r} \rangle = +1$, we get $C^{\text{II}}(r) = [\text{sgn}(J)]^{r-1}$ here. Interestingly, the new factor $[\text{sgn}(J)]^{r-1}$ implies that FC string order is staggered, while AFC string order is not.

Now we construct the picture for type II cluster kink. Since there is no local order parameter, we resort to the fermion language and transform the stabilizer to

$$S_j = \text{sgn}(J) (-1)^m i b_j a_{j+m}, \quad (19)$$

where

$$a_j = c_j + c_j^\dagger, \quad b_j = i(c_j - c_j^\dagger), \quad (20)$$

are Majorana fermions. We can always pair the Majorana fermions coming from different lattice sites, b_j and a_{j+m} , into a new fermion, \tilde{c}_j , so as to get [35]

$$S_j = 1 - 2\tilde{c}_j^\dagger \tilde{c}_j = \begin{cases} +1 & (\tilde{c}_j^\dagger \tilde{c}_j = +1), \\ -1 & (\tilde{c}_j^\dagger \tilde{c}_j = -1), \end{cases} \quad (21)$$

no matter in the FC or AFC cases. Thus the picture of the cluster kink basing on stabilizers is the same as that basing on Majorana fermions. The case for $m = 2$ is illustrated in Fig. 3. One should notice that the uniqueness of the ground state prevents the occurring of spontaneous symmetry breaking.

3. Calculation of the correlation functions

We have defined two correlation functions in Eqs. (14) and (18) for describing symmetry breaking order and string order respectively from the point of view of spin operators. However, their calculations are almost the same in the Majorana fermion language, because we have

$$C^{\text{I}}(r) = (-1)^{\frac{m-1}{2}} \langle b_j a_{j+m} \cdots b_{j+r} a_{j+r+m} \rangle, \quad (22)$$

for the symmetry breaking order ($m \in \text{odd}$), and

$$C^{\text{II}}(r) = (-1)^{\frac{m}{2}} \langle b_j a_{j+m} \dots b_{j+r} a_{j+r+m} \rangle, \quad (23)$$

for the string order ($m \in \text{even}$). The same part, $\langle b_j a_{j+m} \dots b_{j+r} a_{j+r+m} \rangle$, can be decomposed by Wick's theorem and written in a Toeplitz determinant, which facilitates us to evaluate it by further analytical or numerical methods [27, 29].

C. Cluster kink number

Now we define the quantity for calculating number of kinks. For the pure cluster Hamiltonian in Eq. (1), the number of cluster kinks of a given excited state can be counted exactly since the state must be an eigenstate of the stabilizers. We define the number of cluster kinks as

$$\mathcal{N} = \frac{1}{2} \sum_{j=1}^N (1 - \langle S_j \rangle), \quad (24)$$

where $\langle S_j \rangle$ means the value of operator S_j on a given state. Later, we shall demonstrate that the density of cluster kinks,

$$\rho = \frac{\mathcal{N}}{N}, \quad (25)$$

can depict the occurrence of quantum phase transitions. The saturate value of ρ is $1/2$. The Ising case has been used in many previous works [4].

D. The effect of ring frustration

Two properties of the ground states of the Hamiltonian H_m^{xzx} with $J > 0$ (AFC case), the degeneracy D and kink number \mathcal{N} for sequences of m , are summarized in Table I. Basing on it, we shall elucidate the condition for the effect of ring frustration.

If one chooses $m \in \text{even}$, the uniqueness of the ground state won't be changed no matter whether we set $N \in \text{odd}$ or $N \in \text{even}$ in the AFC case. Meanwhile the ground state possesses no kink that can be detected by the stabilizers. Nothing changes when one shifts the oddity of N . Thus there is no effect of ring frustration in these conditions. Another recent study came to the same conclusion [36].

Whereas, the condition, $N \in \text{odd}$ and $m \in \text{odd}$, is the right one for realizing ring frustration. First, the order parameter $\langle \mathcal{O}_j^{xy} \rangle$ takes alternative values, $+1$ and -1 , just like the Ising case [27]. Second, the degeneracy of the ground states increase with the total number of lattice sites, $D = 2N$. From the picture of type I cluster kink in Fig. 2, it is obvious to verify this fact pictorially. In a chain with perfect PBC, only $N - 1$ stabilizers are

| $N \in \text{even}$ | | | $N \in \text{odd}$ | | |
|---------------------|----------|---------------|--------------------|----------|---------------|
| m | D | \mathcal{N} | m | D | \mathcal{N} |
| 1 | 2 | 0 | 2 | 1 | 0 |
| 3 | 2 | 0 | 4 | 1 | 0 |
| 5 | 2 | 0 | 6 | 1 | 0 |
| \vdots | \vdots | \vdots | \vdots | \vdots | \vdots |
| | | | 1 | $2N$ | 1 |
| | | | 3 | $2N$ | 1 |
| | | | 5 | $2N$ | 1 |
| | | | \vdots | \vdots | \vdots |
| | | | 2 | 1 | 0 |
| | | | 4 | 1 | 0 |
| | | | 6 | 1 | 0 |
| | | | \vdots | \vdots | \vdots |

TABLE I. Degeneracy D and kink number \mathcal{N} of the ground states of the pure m -cluster Hamiltonian in Eq. (1) with $J > 0$ (AFC case) for sequences of m . Please note the ground states whose degeneracy reads $D = 2N$ due to the effect of ring frustration under the condition $N \in \text{odd}$ and $m \in \text{odd}$.

independent and the last one is determined by them since we have

$$S_N = - \prod_{j=1}^{N-1} S_j. \quad (26)$$

and the degeneracy reaches as large as $2N$ due to the translational symmetry of the Hamiltonian. All ground states are one-kink states because one stabilizer must take the value -1 . Half of the ground states exhibit one kink and another half exhibit one anti-kink.

Now the system may fall into one of the $2N$ degenerate ground states and break both the \mathbb{Z}_2 symmetry and the translational symmetry. However, in the next section, we will show that quantum fluctuations can lift the degeneracy and lead to unique ground state with restored symmetries, meanwhile, a peculiar extended-kink phase emerges.

E. Further remarks

1. Kramers-Wannier dual transformation

To see the degeneracy of the ground state(s) in a constructive way, we can adopt the discussion basing on the Kramers-Wannier (KW) dual transformation alternatively [20]. The transformation should be designed appropriately according to the oddity of m in order to fulfill the correct Pauli algebra. For $m \in \text{even}$, the transformation should be defined as

$$Z_j = \sigma_{j-1}^x \tau_{m,j}^z \sigma_{j+m-1}^x, \quad X_j = \sigma_j^x, \quad (27)$$

where the dependence of Z_j on m is omitted for abbreviation, so the pure cluster Hamiltonian can be rewritten in a dual form,

$$H_m^{xzx} = J \sum_{j=1}^N Z_j. \quad (28)$$

While for $m \in \text{odd}$, the transformation should be

$$Z_j = \sigma_j^x \tau_{m,j}^z \sigma_{j+m}^x \quad (j \neq N), \quad Z_N = \sigma_N^x \prod_{l=1}^{m-1} \sigma_l^z, \\ X_j = \prod_{k=1}^j \sigma_k^x \left(\prod_{l=k+1}^{k+m-2} \sigma_l^z \right) \sigma_{k+m-1}^x, \quad (29)$$

and we get

$$H_m^{xzx} = J \sum_{j=1}^{N-1} Z_j + J \prod_{j=1}^{N-1} Z_j. \quad (30)$$

Then it is easy to check the degeneracies of the ground states listed in Table I by Eqs. (28) and (30) following the discussion in Ref. [20]. Under the condition for ring frustration, $N \in \text{odd}$ and $m \in \text{odd}$, we see clearly again the degeneracy of the ground states, $D = 2N$.

2. Applicability of cluster kink number

For the pure cluster Hamiltonian Eq. (1), the cluster kinks mainly occur in the excited states, which would be a consequence of thermal fluctuations. However, the kinks can also emerge and pervade in the ground state as a consequence of quantum fluctuations aroused by non-commutative terms added to the Hamiltonian, such as the ones due to a transverse field [2]. We shall demonstrate that the definition of cluster kink number in Eq. (24) is also valid in this situation. Moreover, cluster kinks deriving from different sources can coexist, compete with each other, and induce quantum phase transition. The relation between the kink density and quantum phase transition will be exemplified in Sec. III in detail.

III. MIXED CLUSTER MODEL

In the last section, we pointed out that a general concept of quantum cluster kink can be introduced in the pure cluster model in an exact manner. In this section, we demonstrate that this concept can be used to identify the relevant quantum phase transitions. We also pointed out the effect of ring frustration under the special condition, $N \in \text{odd}$ and $m \in \text{odd}$, in the AFC case. We shall investigate the effect of ring frustration in the ground states by extensively analyzing the kink number, string correlation function, and entanglement spectrum. We will see that the occurrence of quantum phase transition can not be altered by ring frustration, but ring frustration leaves "fingerprint" in the string correlation function and entanglement spectrum as a non-local information.

A. The Hamiltonian

Now we consider the mixed cluster model, [22],

$$H = H_m^{xzx} + H_n^{yzy} + H^z, \quad (31)$$

where H_m^{xzx} can be found in Eq. (1), $H_n^{yzy} = \lambda \sum_{j=1}^N \sigma_j^y \tau_{j,n}^z \sigma_{j+n}^y$ is also a pure cluster model, and $H^z = -g \sum_{j=1}^N \sigma_j^z$ is a term due to transverse field.

By the Jordan-Wigner transformation in Eq. (2), the mixed cluster model is mapped to two fermion Hamiltonians, $H^{(\mp)}$, according to PBC ($c_{N+j} = c_j$) or anti-PBC ($c_{N+j} = -c_j$) boundary condition, which can be cast into the same expression,

$$H^{(\mathcal{P}_z)} = \sum_{j=1}^{N-m} h_j^J - \mathcal{P}_z \sum_{j=1}^m b_j^J + \sum_{j=1}^{N-n} h_j^\lambda \\ - \mathcal{P}_z \sum_{j=1}^n b_j^\lambda + \sum_{j=1}^N h_j^z, \quad (32)$$

where

$$h_j^J = (-1)^m J (c_j - c_j^\dagger) (c_{j+m} + c_{j+m}^\dagger), \\ h_j^\lambda = (-1)^n \lambda (c_j + c_j^\dagger) (c_{j+n} - c_{j+n}^\dagger), \\ b_j^J = (-1)^m J (c_{N-m+j} - c_{N-m+j}^\dagger) (c_j + c_j^\dagger), \\ b_j^\lambda = (-1)^n \lambda (c_{N-n+j} + c_{N-n+j}^\dagger) (c_j - c_j^\dagger), \\ h_j^z = -g (2c_j^\dagger c_j - 1). \quad (33)$$

The definition of \mathcal{P}_z can be found in Eq. (7). By the Fourier transformation,

$$c_j = \frac{1}{\sqrt{N}} \sum_q c_q e^{-iqj}, \quad (34)$$

and the Bogoliubov transformation,

$$\eta_q = u_q c_q - iv_q c_{-q}^\dagger \quad (q \neq 0 \text{ or } \pi), \quad (35)$$

with

$$u_q^2 = \frac{1}{2} \left[1 + \frac{\epsilon(q)}{\omega(q)} \right], \quad v_q^2 = \frac{1}{2} \left[1 - \frac{\epsilon(q)}{\omega(q)} \right], \quad u_q v_q = \frac{\Delta(q)}{\omega(q)}, \\ \epsilon(q) = -(-1)^m J \cos(mq) + (-1)^n \lambda \cos(nq) - h, \\ \Delta(q) = -(-1)^m J \sin(mq) - (-1)^n \lambda \sin(nq), \\ \omega(q) = \sqrt{\epsilon(q)^2 + \Delta(q)^2},$$

the two free fermion Hamiltonians can be diagonalized in the momentum space as,

$$H^{(-)} = \sum_{q \neq 0} \omega(q) (2\eta_q^\dagger \eta_q - 1) + C_0 (2c_0^\dagger c_0 - 1), \\ H^{(+)} = \sum_{q \neq \pi} \omega(q) (2\eta_q^\dagger \eta_q - 1) + C_\pi (2c_\pi^\dagger c_\pi - 1), \quad (36)$$

where $C_0 = (-1)^m J - (-1)^n \lambda - h$, $C_\pi = -J + \lambda - h$. Notice that we have $q \in Q^{(-)}$ for $H^{(-)}$ and $q \in Q^{(+)}$ for $H^{(+)}$ with the definitions,

$$Q^{(-)} = \left\{ -\frac{N-1}{N}\pi, \dots, -\frac{2}{N}\pi, 0, \frac{2}{N}\pi, \dots, \frac{N-1}{N}\pi \right\}, \quad (37)$$

$$Q^{(+)} = \left\{ -\frac{N-2}{N}\pi, \dots, -\frac{1}{N}\pi, \frac{1}{N}\pi, \dots, \frac{N-2}{N}\pi, \pi \right\}. \quad (38)$$

According to QJWM in Eq. (3), we can get the solution of H by the projection,

$$H = P_z^- H^{(-)} + P_z^+ H^{(+)}. \quad (39)$$

All energy states can be parsed after some tedious projection. Please refer to the procedure elaborated in our previous works [27].

B. Ground-state phase diagram

As disclosed in Sec. II, the ring frustration leads to huge ground-state degeneracy as large as $2N$ for the pure cluster model. While for the mixed cluster model here, we can observe that the degeneracy is lifted and, as another landmark of the effect of ring frustration, $2N$ low-lying energy states constituting a gapless band and specifying an extended-kink (EK) phase.

Let us see the ground-state phase diagrams exemplified in Fig. 4. The low energy levels are also plotted, which facilitates us to locate the EK phases. We have fixed the condition, $J > 0$, $m \in \text{odd}$, and $N \in \text{odd}$, so that the first term H_m^{xzx} in Eq. (31) always holds the effect of ring frustration. While for the second term H_m^{yzy} , we consider both odd and even n so as to observe the competition between two types of cluster kinks and explore appropriate quantities to characterize the EK phase.

Three typical examples are presented. In Fig. 4(a), we set the values, $\lambda = 0$ and $m = 3$. We observe two paramagnetic (PM) and one EK phases. The label "x-EK" means that this EK phase derives from the term H_m^{xzx} in Eq. (31). In Fig. 4(b), the parameters are $g = 0$, $m = 3$, and $n = 3$. We get the symmetry breaking (SB), x-EK, and y-EK phases. Notice the SB phase exhibits doubly degenerate ground states and symmetry breaking order [26]. Likewise, the label "y-EK" means that this EK phase derives from the term H_m^{yzy} . In Fig. 4(c), the parameters are $g = 0$, $m = 3$, and $n = 2$. Because this example will be discussed extensively later, we write down it explicitly,

$$\begin{aligned} H &= H_3^{xzx} + H_2^{yzy} \\ &= J \sum_{j=1}^N \sigma_j^x \sigma_{j+1}^z \sigma_{j+2}^z \sigma_{j+3}^x + \lambda \sum_{j=1}^N \sigma_j^y \sigma_{j+1}^z \sigma_{j+2}^y. \end{aligned} \quad (40)$$

For convenience, we set the energy unit, $J = 1$. The three phases include one EK phase and two topological superconducting (TSC) phases [30]. In both TSC and

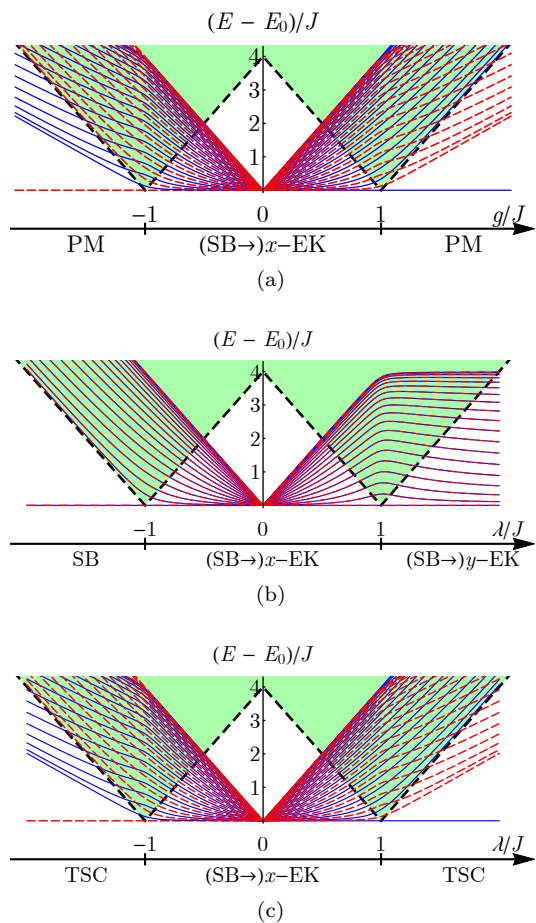


FIG. 4. Phase diagrams of the mixed cluster model with ring frustration ($N \in \text{odd}$ and $m \in \text{odd}$) in different cases: (a) $\lambda = 0$ and $m = 3$; (c) $g = 0$, $m = 3$, and $n = 3$; (b) $g = 0$, $m = 3$, and $n = 2$. The gaplessness in the EK phases occurs in the thermodynamic limit, $N \rightarrow \infty$. Here, we choose $N = 37$ for demonstration. The lowest important $2N$ energy levels are plotted along, which facilitates us to identify the gapless EK phases. The blue lines represent energy levels with odd parity, while the red dashed lines even parity. All other higher levels distribute in the shaded area above the black dashed line. The label "(SB \rightarrow)x/y-EK" means that the EK phase emerges by replacing a gapped SB phase ($N \in \text{even}$, i.e. without ring frustration) in the same parameter range.

PM phases, the ground state is unique. However, the ground-state degeneracy in the EK phases depends. For example, in the case of $g = 0$ and $n = 3$, the ground states are 4-fold degenerate. While in the case of $\lambda = 0$ or $n = 2$, the ground state is unique.

Overall, the ring frustration does not change the number of phases and the occurrence of critical point (the latter will be discussed in the next subsection). The EK phases are just replacements of the SB phases when the system's lattice shifts from $N \in \text{even}$ to $N \in \text{odd}$. But the local order parameter disappears because the absence of symmetry breaking [27].

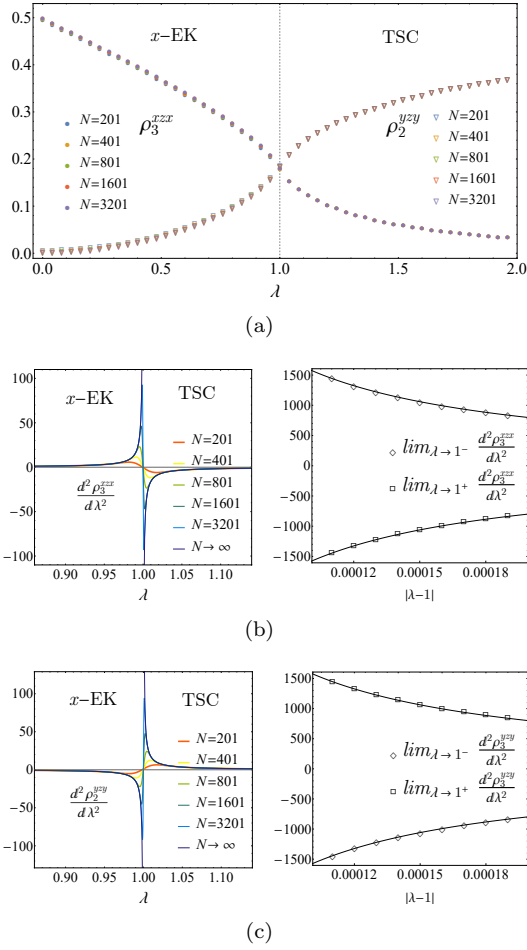


FIG. 5. (a) Kinks densities, ρ_3^{xzx} and ρ_2^{yzy} , in the x -EK and TSC phases. (b) Left: The second derivative of kink density, $\frac{d^2 \rho_3^{xzx}}{d\lambda^2}$; Right: Scaling analysis near the critical point. (c) Left: The second derivative of kink density, $\frac{d^2 \rho_2^{yzy}}{d\lambda^2}$; Right: Scaling analysis near the critical point. Please see the fitting parameters in Eqs. (44) and (45). Here, we choose the sequence of lattice sizes, $N = 201, 401, 801, 1601, 3201$.

C. Kink number and quantum phase transition

1. Second derivative of kink number

In the mixed cluster model, the two pure cluster terms, H_m^{xzx} and H_n^{yzy} , apparently provide two competing types of cluster kinks. Correspondingly, we define two types of kink numbers, \mathcal{N}_m^{xzx} and \mathcal{N}_n^{yzy} (also two types of kink densities, ρ_m^{xzx} and ρ_n^{yzy}), according to Eqs. (24) and (25). Now we demonstrate that quantum phase transition can also be described from the point of view of competing cluster kinks, which gives the same conclusion of the critical point [18, 22].

The idea can be borrowed from the transverse Ising model, which is the limiting case with $\lambda = 0$ and $m = 1$ in the mixed cluster model in Eq. (31). In this limit, the

kink density is in fact the energy density of the ground state, whose second derivative goes divergent at the critical point, $g/J = 1$ [37]. Inspired by this precedent, we hope to use the second derivative of the kink densities, $\frac{d^2 \rho_m^{xzx}}{d\lambda^2}$ (or $\frac{d^2 \rho_n^{yzy}}{d\lambda^2}$), to characterize the phase transitions in the mixed cluster model. We expect the scaling behaviors,

$$\left. \frac{d^2 \rho_m^{xzx}}{d\lambda^2} \text{ (or } \frac{d^2 \rho_n^{yzy}}{d\lambda^2} \right) \Big|_{\lambda \rightarrow \lambda_c \pm \delta} = \text{const} + a_{\pm} |\lambda - \lambda_c|^{-\kappa_{\pm}} + b_{\pm} \log |\lambda - \lambda_c|, \quad (41)$$

at the critical point λ_c , where $\delta = 0^+$ is a infinitesimal and positive real number, $\lambda \rightarrow \lambda_c \pm \delta$ means approaching the critical point from the left or right side, κ_+ and κ_- are corresponding critical exponent. a_{\pm} and b_{\pm} are coefficients and can be obtained by data fitting. Usually, we needn't bother about the last logarithmic term if $\kappa_{\pm} \neq 0$.

To exemplify the idea, we study the Hamiltonian in Eq. (40). Notice that we set $J = 1$ and $N \in \text{odd}$ to impose ring frustration. The phase diagram is depicted in Fig. 4(c). The Hamiltonian has two competing orders, the symmetry breaking order and string order controlled by H_3^{xzx} and H_2^{yzy} respectively. When $-1 < \lambda < 1$, the system is in the x -EK phase, when $\lambda > 1$, the system is in the TSC phase. There is a critical point at $\lambda_c = 1$. Let us observe the critical behaviors,

$$\rho_3^{xzx} = \frac{1}{2N} \sum_{j=1}^N (1 + \langle \sigma_j^x \sigma_{j+1}^z \sigma_{j+2}^z \sigma_{j+3}^x \rangle), \quad (42)$$

$$\rho_2^{yzy} = \frac{1}{2N} \sum_{j=1}^N [1 + \text{sgn}(\lambda) \langle \sigma_j^y \sigma_{j+1}^z \sigma_{j+2}^y \rangle], \quad (43)$$

and their second derivatives. Numerical results are illustrated in Fig. 5. Basing on the data output from a sequence of lattice sizes, $N = 201, 401, 801, 1601, 3201$, we observed the critical behaviors represented by the fitting parameters,

$$a_- = 0.158767, \quad a_+ = -0.15879, \quad \kappa_+ = \kappa_- = 1, \quad (44)$$

for $\frac{d^2 \rho_3^{xzx}}{d\lambda^2}$ and

$$a_- = -0.158744, \quad a_+ = 0.158813, \quad \kappa_+ = \kappa_- = 1, \quad (45)$$

for $\frac{d^2 \rho_2^{yzy}}{d\lambda^2}$ respectively. The values of $|a_{\pm}|$ are very close, so we can safely say that the divergent peaks are anti-symmetric about the critical point (Please see Fig. 5 (b) and (c)). It is noteworthy that the result for another critical point, $\lambda = -1$, is almost the same.

2. Relation between the kink numbers and the ground state energy

There is a direct relation between the kink numbers and the ground state energy of the Hamiltonian in Eq.

(40),

$$\epsilon_0 = 2[\rho_3^{xxx} + \text{sgn}(\lambda) \lambda \rho_2^{yzy}] - [1 + \text{sgn}(\lambda) \lambda], \quad (46)$$

where $\epsilon_0 = E_0/N$ is the ground-state energy density. It is well-known that the second derivative of the ground-state energy density, $\frac{d^2 \epsilon_0}{d\lambda^2}$, can also capture the critical point, $\lambda_c = 1$. However, by the data output from a sequence of lattice sizes, $N = 201, 401, 801, 1601, 3201$, we observed a symmetric logarithmic divergent behavior,

$$\frac{d^2 \epsilon_0}{d\lambda^2} \sim -0.31 \log |\lambda - 1|, \quad (47)$$

which seems to contradict the relation in Eq. (46) since $\frac{d^2 \rho_3^{xxx}}{d\lambda^2}$ and $\frac{d^2 \rho_2^{yzy}}{d\lambda^2}$ are not logarithmic divergent as disclosed in Eqs. (41), (44), and (45). In fact, this interesting consequence reflects the competition between the two types of kinks. Therein the peaks with divergent behavior $|\lambda - \lambda_c|^{-1}$ cancel and meantime the peaks with divergent behavior $\log |\lambda - \lambda_c|$ becomes dominant in $\frac{d^2 \epsilon_0}{d\lambda^2}$.

3. Difference of kink number between with and without ring frustration

However, if we consider the same Hamiltonian in Eq. (40) without ring frustration by setting $N \in \text{even}$, the x -EK phase will be replaced by a SB phase with doubly

degenerate ground states and gapped excitations. But the critical point still holds. Thus the kink density and its second derivative can not tell the difference between the x -EK and SB phases. To see how this happens, we investigate the kink number \mathcal{N}_3^{xxx} for both systems with $N \in \text{odd}$ and $N \in \text{even}$ (i.e. the former exhibits ring frustration, the latter does not). We observe a robust behavior in the difference of kink numbers between them. For the Hamiltonian in Eq. (40), we can write down the result explicitly as

$$\begin{aligned} \Delta \mathcal{N}_3^{xxx} &= \mathcal{N}_3^{xxx}(N \in \text{odd}) - \mathcal{N}_3^{xxx}(N \in \text{even}) \\ &= \begin{cases} 0 & (\lambda < -1, \text{TSC}); \\ 1 & (-1 < \lambda < 1, x\text{-EK}); \\ 0 & (\lambda > 1, \text{TSC}). \end{cases} \end{aligned} \quad (48)$$

This result can be verified by systems with various lattice sizes. In contrast, we can do the same calculation for the kink number \mathcal{N}_2^{yzy} , and get a trivial result,

$$\begin{aligned} \Delta \mathcal{N}_2^{yzy} &= \mathcal{N}_2^{yzy}(N \in \text{odd}) - \mathcal{N}_2^{yzy}(N \in \text{even}) \\ &= \begin{cases} 0 & (\lambda < -1, \text{TSC}); \\ 0 & (-1 < \lambda < 1, x\text{-EK}); \\ 0 & (\lambda > 1, \text{TSC}). \end{cases} \end{aligned} \quad (49)$$

Thus the nontrivial value, $\Delta \mathcal{N}_3^{xxx} = 1$ in the range $-1 < \lambda < 1$, is a good label for the effect of ring frustration.

| | | | |
|--|--|--|--|
| (a) $\lambda = 0$ and $m \in \text{odd}$ | | | |
| | PM ($g/J < -1$) | x -EK ($-1 < g/J < 1$) | PM ($g/J > 1$) |
| $C_m^{I,xxx}(r)$ | 0 | $(-1)^{r+\frac{m}{2}-1} (1 - \frac{h^2}{J^2})^{\frac{m}{4}} (1 - 2\alpha)$ | 0 |
| (b) $g = 0$, $m \in \text{odd}$, and $n \in \text{odd}$ | | | |
| | SB ($\lambda/J < -1$) | x -EK ($-1 < \lambda/J < 1$) | y -EK ($\lambda/J > 1$) |
| $C_m^{I,xxx}(r)$ | 0 | $(-1)^{r+\frac{m}{2}-1} (1 - \frac{\lambda^2}{J^2})^{\frac{m+n}{4}} (1 - 2\alpha)$ | 0 |
| $C_n^{I,yzy}(r)$ | $(-1)^{\frac{n}{2}-1} (1 - \frac{J^2}{\lambda^2})^{\frac{m+n}{4}}$ | 0 | $(-1)^{r+\frac{n}{2}-1} (1 - \frac{J^2}{\lambda^2})^{\frac{m+n}{4}} (1 - 2\alpha)$ |
| (c) $g = 0$, $m \in \text{odd}$, and $n \in \text{even}$ | | | |
| | TSC ($\lambda/J < -1$) | x -EK ($-1 < \lambda/J < 1$) | TSC ($\lambda/J > 1$) |
| $C_m^{I,xxx}(r)$ | 0 | $(-1)^{r+\frac{m}{2}-1} (1 - \frac{\lambda^2}{J^2})^{\frac{m+n}{4}} (1 - 2\alpha)$ | 0 |
| $C_n^{II,yzy}(r)$ | $(-1)^{\frac{n}{2}} (1 - \frac{J^2}{\lambda^2})^{\frac{m+n}{4}}$ | 0 | $(-1)^{r+\frac{n}{2}} (1 - \frac{J^2}{\lambda^2})^{\frac{m+n}{4}}$ |

TABLE II. Correlation functions corresponding to the three typical phase diagrams in Fig. 4. Please notice that there are nonlocal scaling factors, $(1 - 2\alpha)$ with $\alpha = r/N$, in the EK phases, which is a consequence of ring frustration.

D. Correlation function with nonlocal scaling factor

It has been demonstrated that the effect of ring frustration lies in that a nonlocal scaling factor will emerge

in the correlation function [27–29]. To capture the effect in the mixed cluster model, we work out the correlation functions, $C_m^{I,xxx}(r)$ and $C_n^{I/II,yzy}(r)$, according to the definitions in Eqs. (14) and (18). To match the three typical cases of phase diagrams illustrated in Fig.

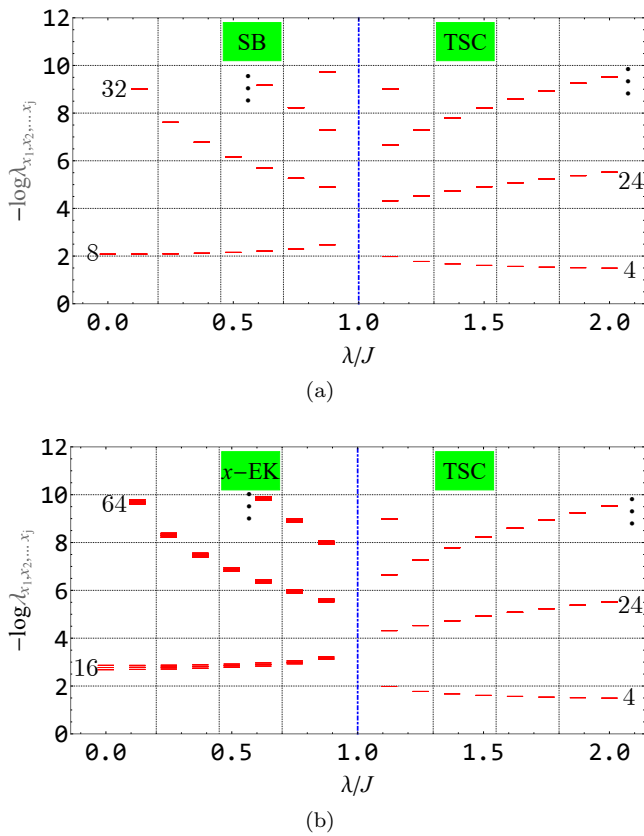


FIG. 6. Entanglement spectrum of the Hamiltonian in Eq. (40) for $N = 3000$ (without ring frustration) (a) and $N = 3001$ (with ring frustration) (b). We expect the eigenvalues are highly degenerate in the thermodynamics. The degeneracies of two lowest eigenvalues are labelled. The result shows that the number of lowest eigenvalues in the EK phase are doubled if ring frustration is imposed.

4, we restore the subscript m, n , superscripts xzx , and zyz to ascribe the sources of orders deriving from H_m^{xzx} and H_n^{zyz} respectively. The analytical results are listed in Table II, which clearly show that the EK phases are captured by the nonlocal scaling factor, $(1 - 2\alpha)$ with $\alpha = r/N$. The emergence of the nonlocal scaling factor marks the absence of symmetry breaking due to the effect of ring frustration [33]. Thus the nonzero correlation function does not mean any local order parameter in the EK phases. Instead, it reflects a nonlocal correlation without local order parameter just like the string correlation function.

E. Entanglement spectrum

In this section, we investigate the important entangled property of ground state in the mixed cluster model by the entanglement spectrum [38, 39]. The reduced density matrix of subsystem l is defined by partial trace as

$$\rho_l = \text{Tr}_{N-l} \rho, \quad (50)$$

where ρ is the full density matrix $|E_0\rangle\langle E_0|$. And the entanglement spectrum of ρ_l is the set of numbers $\lambda_{x_1 x_2 \dots x_j}$ which is defined as [40]

$$\lambda_{x_1 x_2 \dots x_j} = \prod_{j=1}^l \frac{1 + (-1)^{x_j} v_j}{2}, \quad x_j = 0, 1 \quad \forall j. \quad (51)$$

where v_j is the imaginary part of the eigenvalues of the correlation matrix [41].

Now we give the numerical results for the Hamiltonian in Eq. (40). To display the effect of ring frustration, we illustrate the results without and with ring frustration ($N = 3000$ and 3001 respectively). When the system's size shifts from $N = 3000$ to $N = 3001$, SB phase is replaced by x -EK phase in the parameter range $0 < \lambda/J < 1$. More important, we observe that the number of lowest eigenvalues in the spectrum is doubled when ring frustration is imposed. This phenomena can be taken as a fingerprint of ring frustration in the entanglement spectrum.

IV. SUMMARY AND DISCUSSION

In summary, we have introduced the general concept of quantum cluster kink and pointed out the condition for realizing ring frustration in the pure and mixed cluster models. And as we have uncovered, there are two types of cluster kinks corresponding to two types of ground states, of which one has symmetry-breaking order and another nonlocal string order. Ring frustration can be realized in the type with symmetry-breaking order, which results in the EK phase without symmetry breaking. Cluster kinks deriving from different sources can coexist, compete with each other, and lead to quantum phase transition. Although the ring frustration does not change the phase transition point, it will bring a nonlocal scaling factor to the correlation function and double the degeneracy of the entanglement spectrum of the ground state in the EK phase.

From these peculiar conclusions, we see that ring frustration can provide us a brand new way to explore controllable interesting quantum extended-kink states with long-range correlation function but without symmetry breaking. As an order-induced phenomenon, the effect of ring frustration is reminiscent of the one in the well-known spin ladders [42], which is rooted in the exotic parity structure of quantum states.

Nevertheless, there remain some uncovered aspects in such systems. First, for example, we can not cut the ring to maintain the effect of ring frustration, so the usual framework of bulk-edge correspondence that relates the bulk's nontrivial topology to the number of edge states [43] is not applicable here. Instead, one can resort to the bulk-defect correspondence [33], but the general conclusion for the cluster model especially with high winding numbers [13, 18, 22] is still lacking. Second, as a pending issue, the dynamics of cluster kinks is an interesting topic

to go on with, since the general cluster kink exhibits a quantum nature compared with the classical Ising kink [3, 4]. Third, the definition of cluster kink relies on the specific terms in the Hamiltonian, so one would like to know whether it is applicable in other models without

such terms like the ubiquitous Ising kink.

ACKNOWLEDGMENTS

This work is supported by NSFC under Grants No. 11074177.

-
- [1] N. Nagaosa, *Quantum Field Theory in Condensed Matter Physics* (Springer, 1999).
- [2] S. Sachdev, *Quantum Phase Transitions, 2nd ed* (Cambridge University Press, 2011).
- [3] W. H. Zurek, U. Dorner, and P. Zoller, Dynamics of a quantum phase transition, *Phys. Rev. Lett.* **95**, 105701 (2005).
- [4] J. Dziarmaga, Dynamics of a quantum phase transition: Exact solution of the quantum ising model, *Phys. Rev. Lett.* **95**, 245701 (2005).
- [5] L. Cincio, J. Dziarmaga, M. M. Rams, and W. H. Zurek, Entropy of entanglement and correlations induced by a quench: Dynamics of a quantum phase transition in the quantum ising model, *Phys. Rev. A* **75**, 052321 (2007).
- [6] A. del Campo, Universal statistics of topological defects formed in a quantum phase transition, *Phys. Rev. Lett.* **121**, 200601 (2018).
- [7] Z. Xu and A. del Campo, Probing the full distribution of many-body observables by single-qubit interferometry, *Phys. Rev. Lett.* **122**, 160602 (2019).
- [8] M. N. Najafi and M. A. Rajabpour, Formation probabilities and statistics of observables as defect problems in free fermions and quantum spin chains, *Phys. Rev. B* **101**, 165415 (2020).
- [9] A. Milsted, J. Liu, J. Preskill, and G. Vidal, Collisions of false-vacuum bubble walls in a quantum spin chain, arXiv , 2012.07243v1 (2020).
- [10] P. Coleman, *Introduction to Many-Body Physics* (Cambridge University Press, 2015).
- [11] J. K. Pachos and M. B. Plenio, Three-spin interactions in optical lattices and criticality in cluster hamiltonians, *Phys. Rev. Lett.* **93**, 056402 (2004).
- [12] P. Smacchia, L. Amico, P. Facchi, R. Fazio, G. Florio, S. Pascazio, and V. Vedral, Statistical mechanics of the cluster ising model, *Phys. Rev. A* **84**, 022304 (2011).
- [13] G. Zhang and Z. Song, Topological characterization of extended quantum ising models, *Phys. Rev. Lett.* **115**, 177204 (2015).
- [14] S. M. Giampaolo and B. C. Hiesmayr, Genuine multipartite entanglement in the cluster-ising model, *New Journal of Physics* **16**, 093033 (2014).
- [15] S. M. Giampaolo and B. C. Hiesmayr, Topological and nematic ordered phases in many-body cluster-ising models, *Phys. Rev. A* **92**, 012306 (2015).
- [16] G. Zonzo and S. M. Giampaolo, n-cluster models in a transverse magnetic field, *Journal of Statistical Mechanics: Theory and Experiment* **2017**, 63103 (2018).
- [17] S. Bhattacharjee and A. Dutta, Dynamical quantum phase transitions in extended transverse ising models, *Phys. Rev. B* **97**, 134306 (2018).
- [18] W. Nie, F. Mei, L. Amico, and L. C. Kwek, Scaling of geometric phase versus band structure in cluster-ising models, *Phys. Rev. E* **96**, 020106 (2017).
- [19] T. Scaffidi, D. E. Parker, and R. Vasseur, Gapless symmetry-protected topological order, *Phys. Rev. X* **7**, 041048 (2017).
- [20] R. Verresen, R. Moessner, and F. Pollmann, One-dimensional symmetry protected topological phases and their transitions, *Phys. Rev. B* **96**, 165124 (2017).
- [21] Y.-R. Zhang, Y. Zeng, H. Fan, J. Q. You, and F. Nori, Characterization of topological states via dual multipartite entanglement, *Phys. Rev. Lett.* **120**, 250501 (2018).
- [22] C. Ding, Phase transitions of a cluster ising model, *Phys. Rev. E* **100**, 042131 (2019).
- [23] K. Choo, C. W. von Keyserlingk, N. Regnault, and T. Neupert, Measurement of the entanglement spectrum of a symmetry-protected topological state using the ibm quantum computer, *Phys. Rev. Lett.* **121**, 086808 (2018).
- [24] D. Azses, R. Haenel, Y. Naveh, R. Raussendorf, E. Sela, and E. G. Dalla Torre, Identification of symmetry-protected topological states on noisy quantum computers, *Phys. Rev. Lett.* **125**, 120502 (2020).
- [25] V. V. W. Son, L. Amico, Topological order in 1d cluster state protected by symmetry, *Quantum Inf Process* **11**, 1961 (2012).
- [26] C. X. Z. D.-L. W. X.-G. Zeng, B., *Quantum Information Meets Quantum Matter* (Springer, 2019).
- [27] J.-J. Dong, P. Li, and Q.-H. Chen, The a-cycle problem for transverse Ising ring, *Journal of Statistical Mechanics: Theory and Experiment* **11**, 113102 (2016).
- [28] J.-J. Dong, Z.-Y. Zheng, and P. Li, Rigorous proof for the nonlocal correlation function in the transverse Ising model with ring frustration, *Phys. Rev. E* **97**, 012133 (2018).
- [29] P. Li and Y. He, Ring frustration and factorizable correlation functions of critical spin rings, *Phys. Rev. E* **99**, 032135 (2019).
- [30] Z.-Y. Zheng, H.-C. Kou, and P. Li, Quaternary Jordan-Wigner mapping and topological extended-kink phase in the interacting Kitaev ring, *Phys. Rev. B* **100**, 235127 (2019).
- [31] V. Marić, S. M. Giampaolo, D. Kuić, and F. Franchini, The frustration of being odd: how boundary conditions can destroy local order, *New Journal of Physics* **22**, 083024 (2020).
- [32] G. Torre, V. Marić, F. Franchini, and S. M. Giampaolo, Effects of defects in the XY chain with frustrated boundary conditions, *Phys. Rev. B* **103**, 014429 (2021).
- [33] H.-C. Kou, Z.-Y. Zheng, and P. Li, Impurity-driven transitions in frustrated quantum Ising rings, *Phys. Rev. E* **103**, 032129 (2021).
- [34] A. Kitaev, in *Exact Methods in Low-dimensional Statistical Physics and Quantum Computing*, edited by J. Jacobsen, S. Ouvry, V. Pasquier, D. Serban, and L. Cuglian-

- dolo (Oxford University Press, Oxford, 2010).
- [35] A. Y. Kitaev, Unpaired Majorana fermions in quantum wires, *Physics Uspekhi* **44**, 131 (2001).
 - [36] V. Marić, F. Franchini, D. Kuiuć, and S. M. Giampaolo, Resilience of the topological phases to frustration, *Scientific Reports* **11**, 6508 (2021).
 - [37] S. Suzuki, J.-i. Inoue, and B. K. Chakrabarti, *Quantum Ising Phases and Transitions in Transverse Ising Models* (Springer, Berlin, Heidelberg, 2013, 2013).
 - [38] H. Li and F. D. M. Haldane, Entanglement Spectrum as a Generalization of Entanglement Entropy: Identification of Topological Order in Non-Abelian Fractional Quantum Hall Effect States, *Phys. Rev. Lett.* **101**, 010504 (2008).
 - [39] F. Pollmann, A. M. Turner, E. Berg, and M. Oshikawa, Entanglement spectrum of a topological phase in one dimension, *Phys. Rev. B* **81**, 064439 (2010).
 - [40] J. I. Latorre, E. Rico, and G. Vidal, Ground state entanglement in quantum spin chains, arXiv e-prints , quant-ph/0304098 (2003).
 - [41] G. Vidal, J. I. Latorre, E. Rico, and A. Kitaev, Entanglement in quantum critical phenomena, *Phys. Rev. Lett.* **90**, 227902 (2003).
 - [42] E. Dagotto and T. M. Rice, Surprises on the way from one- to two-dimensional quantum magnets: The ladder materials, *Science* **271**, 618 (1996).
 - [43] C.-K. Chiu, J. C. Y. Teo, A. P. Schnyder, and S. Ryu, Classification of topological quantum matter with symmetries, *Rev. Mod. Phys.* **88**, 035005 (2016).